PERGAMON

International Journal of Heat and Mass Transfer 42 (1999) 3619–3629

International Journal of HEAT and MASS TRANSFER

www.elsevier.com/locate/ijhmt

Experimental study of a double-diffusive two-layer system in a laterally heated enclosure

Josef Tanny*, Bachtiyar Yakubov

Center for Technological Education Holon, Holon Institute of Technology Arts and Sciences, POB 305, Holon 58102, Israel

Received 11 August 1998; received in revised form 22 December 1998

Abstract

An experimental study was carried out to investigate the mixing process of a two-layer stratified fluid in a laterally heated enclosure. Due to the lateral heating of the enclosure, a circulating flow is induced in each layer such that the interface separating the layers is simultaneously exposed to destabilizing shear and double diffusive convection. The main goal of this work is to investigate the role of the interfacial instabilities in the mixing process of the two-layer system. The experiments were carried out in a box with inner dimensions of $10 \times 10 \times 10$ cm. Two sidewalls of the box were made of stainless steel and served as heat exchangers, and the two other sidewalls were made of optical glass to facilitate flow visualization. The criterion for the onset of interfacial instabilities and the mixing time of the system were studied experimentally. The results show that when the flow adjacent to the interface is unstable, it is characterized by intense vortices and the mixing time is relatively short. On the other hand, when the interfacial flow is stable, no vortices exist at the interface and the mixing time is much longer.

1. Introduction

Double-diffusive convection phenomena can arise in fluids due to the presence of gradients of two properties, with different molecular diffusivity, which make opposite contributions to the density distribution within the fluid. For a comprehensive review of double-diffusive convection see Turner [1,2], Huppert and Turner [3] and Turner [4].

One of the fundamental double-diffusive systems is a two-layer solute-stratified fluid in a laterally heated enclosure. The interest in this system stems mainly from the fact that the interface separating the layers is a basic element of more complicated double diffusive multi-layered systems. For example, when a continuous stable solute gradient is subjected to a lateral temperature gradient [5] an array of convective layers separated by density interfaces is formed. Under certain conditions the layers undergo a sequence of merging events in each of which two adjacent layers merge into one thicker layer. Merging processes in such a system were studied by, e.g., Wirtz and Reddy [6], Tanny and Tsinober [7,8], Schladow, Thomas and Koseff [9] and Kranenborg and Dijkstra [10].

Evidently, the merging process is controlled by the conditions at the interface separating the layers. Consequently, several research works were focused on the behavior of a single salinity interface in a laterally heated fluid. Bergman and Ungan [11] studied experimentally the behavior of a two-layer system destabilized by lateral heating and cooling in a box. They have identified several stages in the evolution of the system towards complete mixing. Initially, the two nearly uni-

* Corresponding author. Tel.: +972-3-5026-661; fax: +972-3-5026-650.

E-mail address: tanai@barley.cteh.ac.il (J. Tanny)

0017-9310/99/$ - see front matter
PII: S0017-9310(99)00036-8

Nomenclature

A_r	H/L—aspect ratio of the enclosure
ΔC	initial concentration difference between the two layers
D	coefficient of solute diffusivity
g	acceleration due to gravity
H	height of the fluid
L	width of the enclosure
Ra	$g\alpha\Delta TL^3/\nu\kappa$ — Rayleigh number
R_ρ	$\beta\Delta C/\alpha\Delta T$ — buoyancy ratio
t	dimensional time
ΔT	lateral temperature difference

Greek symbols

α	coefficient of thermal expansion
β	coefficient of solutal contraction
κ	coefficient of heat diffusivity
ν	kinematic viscosity
τ	non-dimensional time

Subscripts

c	critical
m	mixing
1	top layer
2	bottom layer

form layers are thermally driven and behave somewhat independently. As salt is transferred across the interface, the stabilizing effect of the salinity difference is decreased and complicated flow structure is observed at the interface. In the final stage the stabilizing salinity gradient becomes small, which allows the thermal boundary layers at the heated and cooled side walls to penetrate the interface and mix the whole system. Bergman and Ungan [11] pointed out that the interface is simultaneously exposed to shear instability due to the circulation in each layer, and to double-diffusive instability due to the stabilizing and destabilizing vertical solute and temperature gradients, respectively. Using the liquid-crystal flow visualization technique, they observed waves which may be induced by shear instability at the interface, and a central vortex, just before the system was completely mixed.

Quantitatively, Bergman and Ungan [11] measured the mixing time associated with layer merging and correlated the time-averaged interfacial salt transport with the non-dimensional parameters governing the problem. In particular, they have shown that for a given buoyancy ratio (defined as the ratio between the stabilizing density step due to salinity and the lateral destabilizing density difference due to temperature), the non-dimensional mixing time decreases as the lateral thermal Rayleigh number is increased. For a given thermal Rayleigh number, the mixing time increases with the buoyancy ratio. The time-averaged interfacial salt transport was found to increase with the thermal Rayleigh number.

Recently, Hyun and Bergman [12] reported a numerical simulation of the above phenomenon. The results indicated two mechanisms that lead to the destruction of the salinity interface. At low lateral thermal Rayleigh numbers thermal convection erodes saline water from the interface and folds it into the convective layer. At higher Rayleigh numbers, salt plumes are torn from the interface, carried by the thermal convection and then, reinforced by the thermal buoyancy, they bombard the interface. The mixing time estimated on the basis of the simulation was in approximate agreement with that measured in experiments performed by Hyun and Bergman [12].

Using the shadowgraph technique Kamakura and Ozoe [13] were able to observe the appearance of waves at the interface, followed by rapid mixing of the two layers. In their experiments, as well as in the experiments by Bergman and Ungan [11], the interface was observed to migrate upwards with time. Kamakura and Ozoe [14] suggested that the observed upward migration of the interface is due to the variation of fluid properties with temperature; a numerical simulation they performed for a fluid with temperature-dependent properties supported this conjecture.

From the above review it appears that in the existing

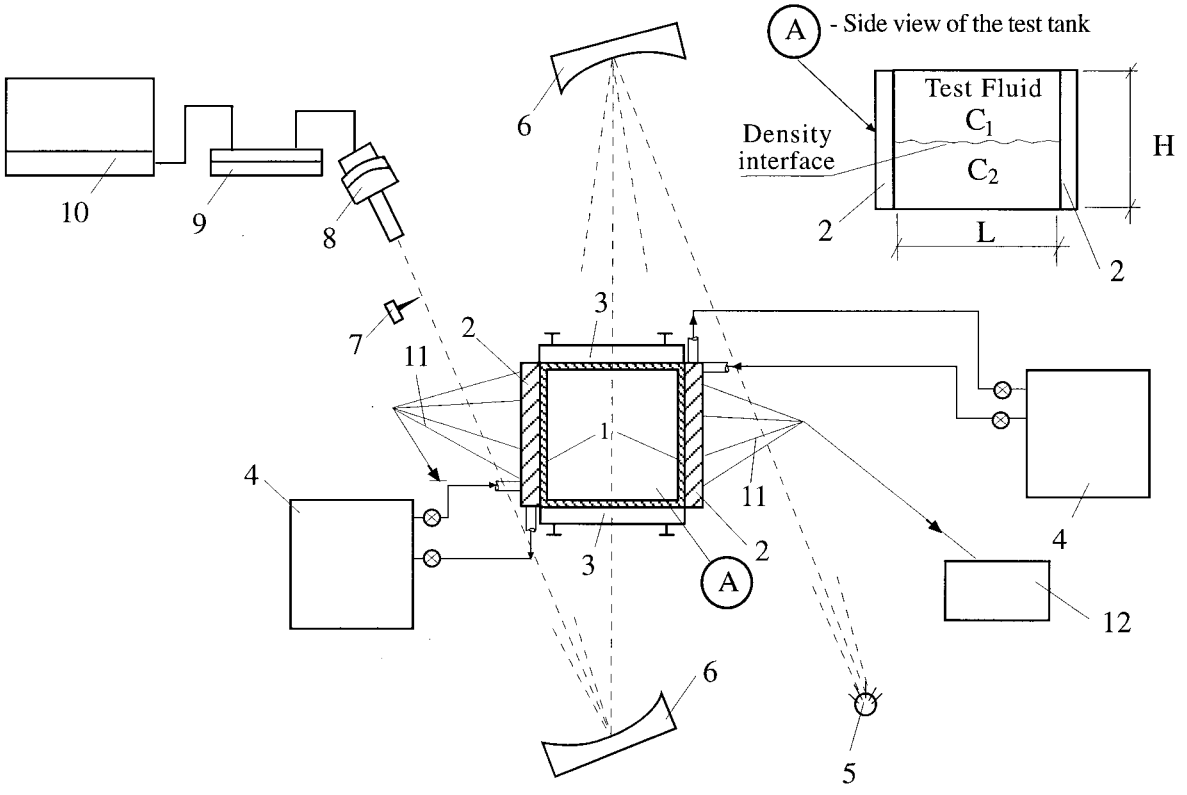

Fig. 1. A schematic view of the experimental apparatus.

literature various mechanisms were suggested for the mixing process of the two-layer stratified fluid. These mechanisms include waves or plumes at the interface, interface migration and penetration of wall boundary layers. However, the effect of interfacial instabilities on the mixing process was not addressed. The aim of the present work is to investigate the criterion for the onset of instabilities at the interface, and to study their role in the mixing process. We first illustrate the qualitative effect of these instabilities on the mixing process by discussing two experiments, under different physical conditions. Then we present the criterion for the onset of the interfacial vortices and the mixing time of the system.

2. Experimental set-up and procedures

The experimental apparatus is shown in Fig. 1. In the following, the numbers in parentheses, indicate the item number in Fig. 1. The experiments were carried out in a box with inner dimensions of $10 \times 10 \times 10$ cm. Two side walls (1) of the box were made of stainless steel and were provided with passages (2) through which water from two constant-temperature baths (4) could circulate. The two other side walls were made of optical glass to facilitate schlieren flow visualization. The metal side walls and the top and base of the box were insulated using Styrofoam plates. The optical glass side walls were insulated by transparent thermal insulation units (3), each consisting of air-filled, optical glass box. The temperature of each side wall was measured by five miniature thermocouples (11) type T, inserted into holes from the back side of the metal wall. The output of the thermocouples was recorded and linearized every 2 min during the experiment, using a data acquisition system (12) consisting of an A/D card, a multiplexer and a 486 PC.

The flow was visualized using a Schlieren system consisting of two spherical mirrors (6), 15.24 cm in diameter and 152.4 cm in focal length, a white light source (5) and a knife edge (7). The system was set up such that the circular parallel beam was passed horizontally through the tank. The output of the schlieren system was imaged by a CCD camera (8), and was displayed on a monitor (10) and also recorded by a time-lapse VCR (9) for later reviewing.

In a few experiments, vertical concentration and temperature profiles were measured by a micro-scale conductivity/temperature instrument (MSCI, Precision

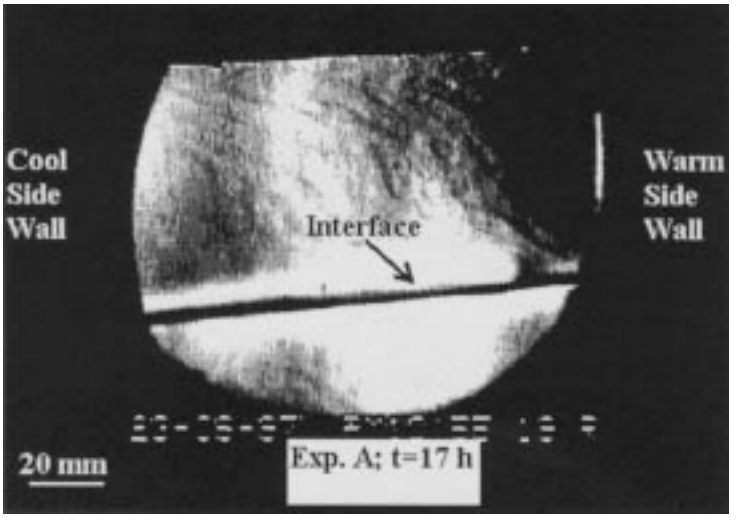

Fig. 2. A Schlieren view of the stable interface in experiment A. A similar view was obtained during earlier stages of this experiment. The interface is slightly inclined due to the lateral temperature difference.

Measurement Engineering, CA, USA). The sensor was traversed vertically through the stratified fluid at a constant speed of 0.025 cm/s, measuring the conductivity and temperature each 0.125 cm. This resulted in 64 data points over 8 cm out of the total fluid depth of 9.2 cm. Data were always recorded while the probe was traversed downwards, with the sensor ahead of the probe holder, to minimize any disturbance at the measured region. The measurements were done at the center of the box, i.e., at a distance of 5 cm from the cool or warm side-walls. The MSCI was calibrated before each experiment against aqueous solutions of five different concentrations and two different temperatures. The output voltage of the sensor was translated to concentration using the local measured temperature and the relations for aqueous NaCl solution given by Head [15].

The two-layer stratified system was established by initially filling the tank with a lower layer of aqueous salt (NaCl) solution of the higher concentration. Then, an upper layer of fresh water was poured carefully (using a wooden float). The two layers had the same depth of 4.6 cm. After filling the tank, the system was allowed to rest for about 5 min before the start of the experiment.

The lateral prescribed temperature difference was applied almost instantaneously by raising and lowering the temperatures of the side walls, and was kept constant throughout the experiment. The temperature of each side wall was found to be uniform within $\pm 0.5^{\circ}$C. Each experiment continued until the two-layer stratified fluid was mixed through the 'catastrophe' stage (see Section 3.2).

3. Results and discussion

3.1. Governing parameters

Before describing the experimental results, we introduce the non-dimensional parameters that govern the flow under study. The lateral temperature difference, ΔT, is represented by the thermal Rayleigh number:

$$Ra = \frac{g\alpha \Delta T L^3}{\nu \kappa}, \tag{1}$$

where g is the acceleration due to gravity, α is the coefficient of thermal expansion, L is the box width (distance between warm and cool side walls, see Fig. 1), ν is the kinematic viscosity and κ is the coefficient of thermal diffusion. The ratio between the stabilizing effect of solute concentration and the destabilizing effect of the temperature gradient is represented by the overall buoyancy ratio:

$$R_\rho = \frac{\beta \Delta C}{\alpha \Delta T} \tag{2}$$

where β is the coefficient of solutal expansion and $\Delta C = C_2 - C_1$ (see Fig. 1) is the initial concentration difference between the two layers.

The geometry of the problem is governed by the aspect ratio of the box, $A_r = H/L$, where H is the height of the fluid. The present experiments were carried out with two layers of equal thickness (4.6 cm each) such that $H = 9.2$ cm and $A_r = 0.92$.

The physical properties of the fluid were estimated at the mean temperature and concentration in the sys-

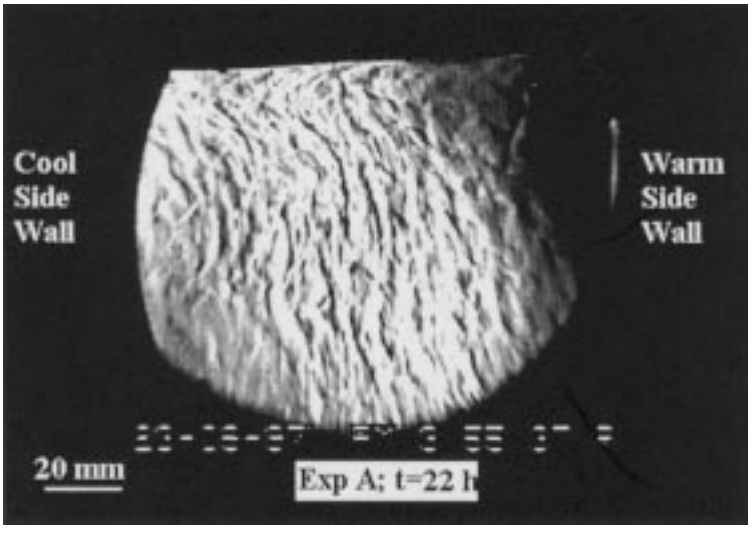

Fig. 3. A Schlieren view of the field of salt-fingers at the 'catastrophe' stage at the end of experiment A.

tem, using the data given in Ruddick and Shirtcliffe [16], Weast [17] and Batchelor [18].

3.2. Qualitative observations

To illustrate the role of the instability phenomena in the mixing process, we present characteristic flow patterns observed during two experiments with the same concentration difference, $\Delta C = 0.2\%$wt, but with different lateral temperature differences, $\Delta T = 2°C$ and $10°C$ (hereafter denoted as experiments A and B, respectively). The corresponding values of the non-dimensional parameters for these experiments are: $Ra_A = 3.96 \times 10^7$, $R_{\rho A} = 2.71$ and $Ra_B = 1.75 \times 10^8$, $R_{\rho B} = 0.59$.

In experiment A, a slow circulating flow within each layer could be observed by the schlieren technique. The interface region was stable and only after 16 h a very faint disturbance could be sometimes observed moving along the interface. A photograph illustrating the interface approximately at this time (17 h) is shown in Fig. 2. The interface is observed to be stable since the disturbance was so faint that it could not be reproduced on the hardcopy. After about 19 h, rows of faint disturbances could be sometimes observed,

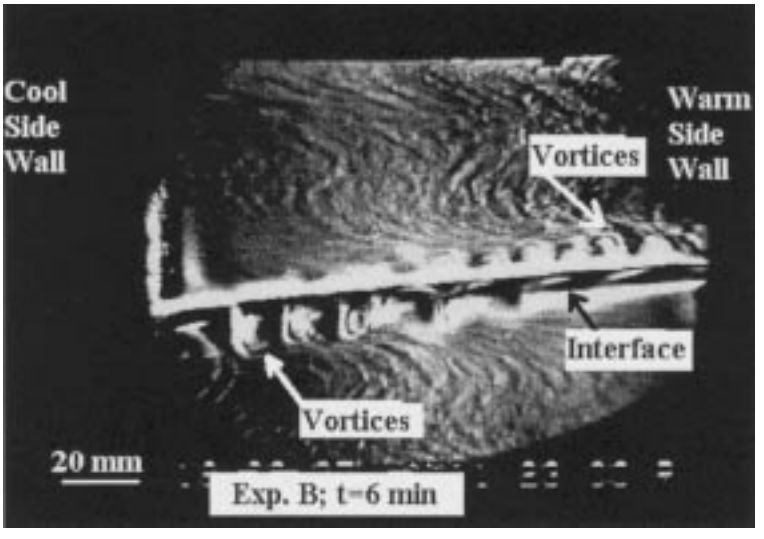

Fig. 4. The vortices at the interface in experiment B. The vortices above the interface move to the right, towards the warm sidewall while the vortices below the interface move towards the left sidewall. The motion of the vortices is caused by the circulating flow within each layer.

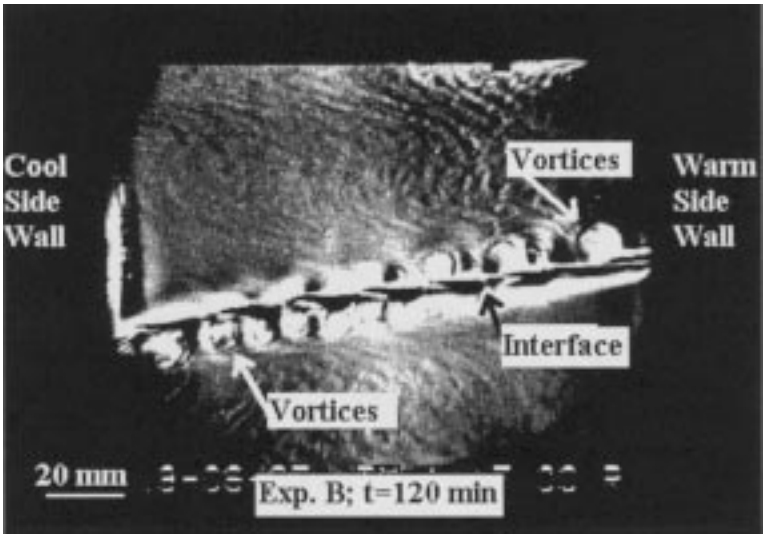

Fig. 5. Vortices at the interface in a later stage of experiment B. In this experiment, the interfacial vortices persisted throughout the experiment.

and the two layers were mixed, through a 'catastrophe' stage, after about 22 h. The 'catastrophe' stage was characterized by the breakdown of the interface near the warm sidewall, followed by a relatively rapid downwards migration of the interface. Along with the interface migration, salt fingers gradually filled the box, as shown in Fig. 3.

In experiment B, on the other hand, instability in the form of well organized, intense vortices was observed about 6 min after the start of heating and cooling (see Fig. 4). The vortices were moving along the interface and persisted throughout the experiment as shown in Fig. 5 at 120 min. In experiment B, the lateral temperature difference was larger than that in experiment A. The increased temperature difference simultaneously affects the two instability mechanisms operating in the system. First, it intensifies the circulating flow within each layer, thus increasing the velocity gradients across the interface and across each layer. The increased vertical gradients of the horizontal velocity can drive interfacial shear instability. The second effect of the lateral temperature difference is to increase

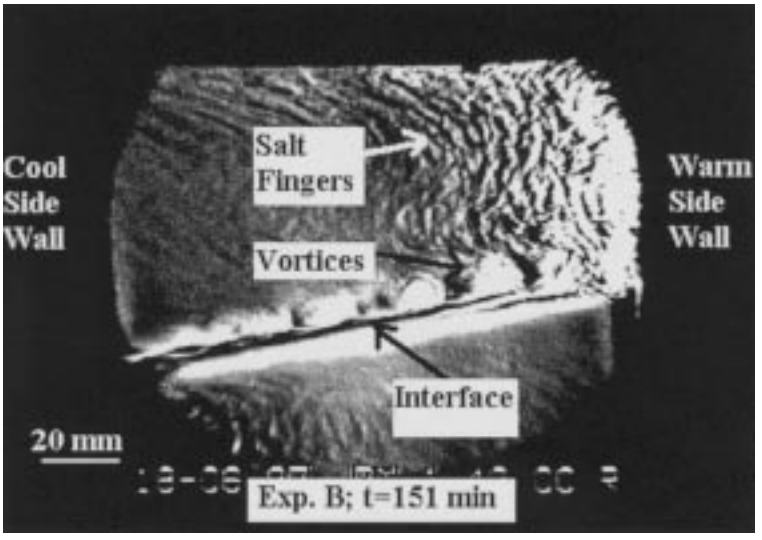

Fig. 6. The onset of the final 'catastrophe' stage in experiment B. The vortices disappeared from the lower part of the interface and salt-fingers start to fill the upper layer.

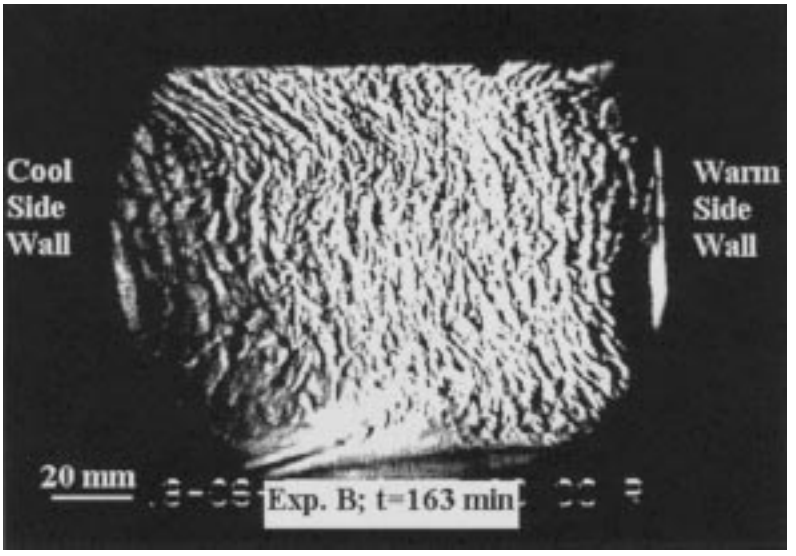

Fig. 7. The field of salt-fingers as observed by the Schlieren technique after the interface migrated downwards at the end of experiment B. A remnant of the interface can be observed at the lower part of the picture.

the vertical temperature gradient across the interface. The interfacial layer is exposed to vertical stabilizing and destabilizing concentration and temperature gradients respectively. When the latter becomes large enough, double diffusive instability can occur. The interfacial vortices observed in Figs. 4 and 5 are generated by these shear and double diffusive instability mechanisms. The motion of the vortices above and below the interface in opposite directions is caused by the circulating flow in each layer.

The 'catastrophe' in experiment B started at about 145 min. At this stage, fluid from the bottom layer penetrated through the interface, near the warm sidewall, into the upper layer, as shown in Fig. 6. This event had two significant effects on the flow field: (i) the circulation in the bottom layer almost ceased and hence, the vortices at the lower side of the interface disappeared; (ii) the fluid penetrating from the bottom layer, which is saltier, but warmer and hence lighter than the top-layer fluid, reached the top of the upper layer. This situation was conducive to the formation of salt-fingers in the right side of the upper layer, as observed in Fig. 6. The 'catastrophe' in experiment B almost completed at $t=163$ min, when the interface migrated downwards, the two layers mixed, and salt fingers filled the whole box, in a similar way as in experiment A. The field of salt fingers at the end of experiment B is shown in Fig. 7.

3.3. Concentration and temperature profiles

In order to illustrate the structure of the flow, we show a few examples of concentration and temperature profiles measured in an experiment in which no vortices existed at the interfacial region. The physical conditions of this experiment were: $Ra=2.91\times10^{8}$, $R_\rho=6.55$. The initial concentrations of the top and bottom layers were 0 and 4%wt, respectively. The temperatures of the cool and warm sidewalls were 9.7 and 28.6°C, respectively, and were kept constant during the experiment which lasted 37 h.

Fig. 8a–c shows vertical concentration (left) and temperature (right) profiles at $t=892$, 1199 and 1495 min, respectively. It is observed that the concentration is uniform within each layer, indicating on the efficient mixing of the circulating flow in each of the layers. The concentration difference decreases with time due to upward transport of salt across the double-diffusive interface. The temperature is essentially linear in each layer, reflecting the natural convection circulating flow in each layer. Both temperature and concentration profiles suggest that at this stage of the experiment the interface migrated upwards. However, the final 'catastrophe' stage was associated with a downwards migration of the interface, as observed in experiment A above.

3.4. The criterion for the onset of the interfacial vortices

Due to the upwards salt transport, the concentration difference across the interface, and hence R_ρ, decreases with time, as was observed in Fig. 8. Thus, every experiment which starts without vortices (like experiment A above) can eventually reach unstable conditions, and vortices may appear at a later stage during the experiment. Indeed, this was the situation in part of the

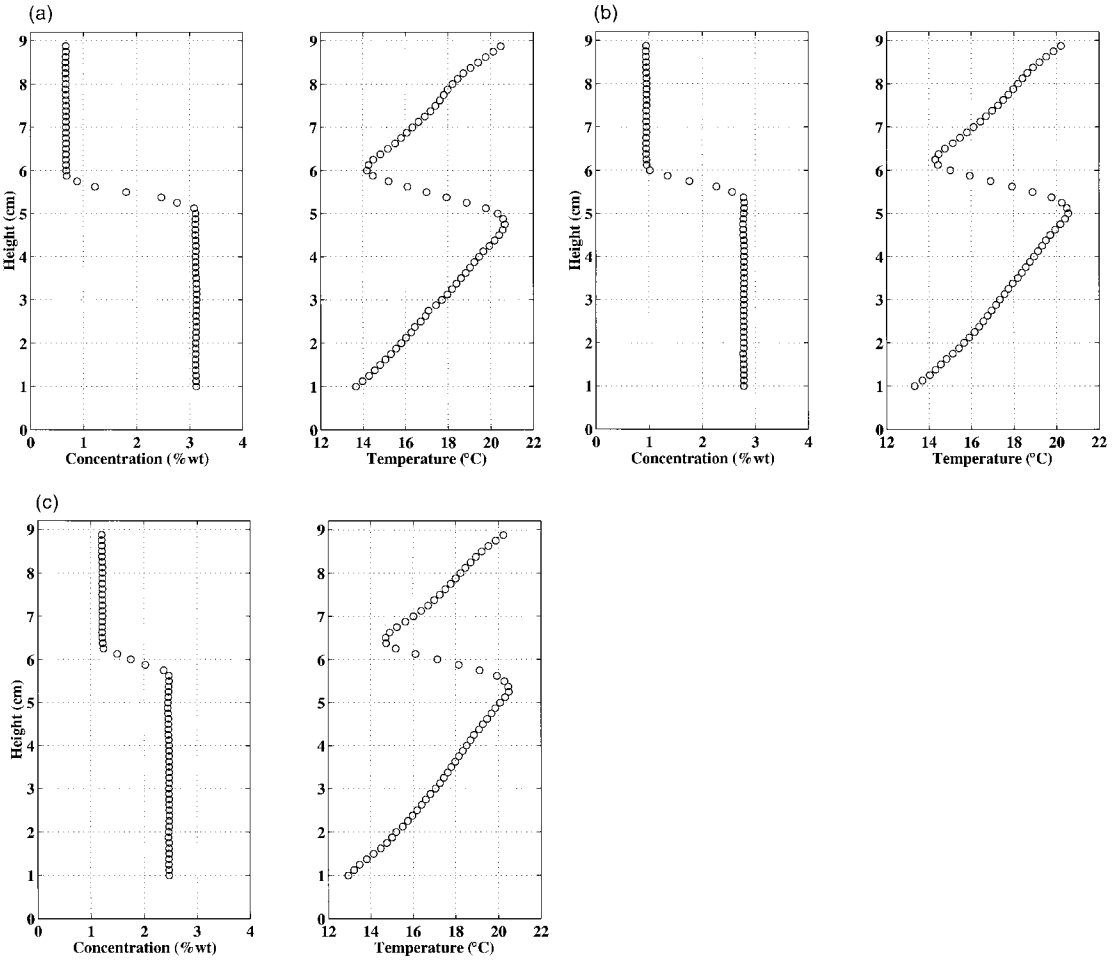

Fig. 8. Examples of vertical concentration (left) and temperature (right) profiles of the two layer stratified fluid. Experimental conditions are: $\Delta C = 4\%$wt, $\Delta T = 18.9°C$, $Ra = 2.91 \times 10^8$, $R_\rho = 6.55$. (a) $t = 892$ min; (b) $t = 1199$ min; (c) $t = 1495$ min.

experiments performed in this study. In the following, however, we distinguish between stable and unstable experiments, according to the *initial* conditions in the experiment and therefore, the buoyancy ratio, R_ρ, is estimated using the initial value of ΔC.

The observations described in Section 3.2. suggest that the appearance of vortices at the start of the experiment depends on the values of the governing parameters. We performed a series of 27 experiments with various conditions to study this phenomenon. The results are presented in Fig. 9 where, for each experiment, the value of Ra is plotted as a function of the initial value of R_ρ. The experiments can be classified into two major categories: *unstable* experiments with vortices (marked x) and *stable* experiments without vortices (marked o). In few experiments, denoted as *transition* (marked +), only very faint vortices appeared at the interface for short periods of time during the experiment. One experiment was performed with a very small $R_\rho = 0.27$ (*highly unstable*, marked *) and was characterized by a very rapid overturning of the interface without the appearance of vortices.

As suggested above, the appearance of vortices at the interface is an instability phenomenon. The criterion of this instability can be deduced by identifying the boundary between stable (*no vortices*) and unstable (*vortices*) experiments. The solid line in Fig. 9, indicating this boundary, has a slope of 1.28, suggesting that the criterion is:

$$Ra_c = 10^{8.2} \times R_\rho^{1.28}. \tag{3}$$

It is observed in Fig. 9 that for a given buoyancy ratio, R_ρ, the interfacial flow can be stable or unstable, depending only on the value of Ra. This observation implies on the role of the shear instability mode, since the lateral ΔT ($\propto Ra$) induces the circulating flow in each layer. On the other hand, it is observed that for a

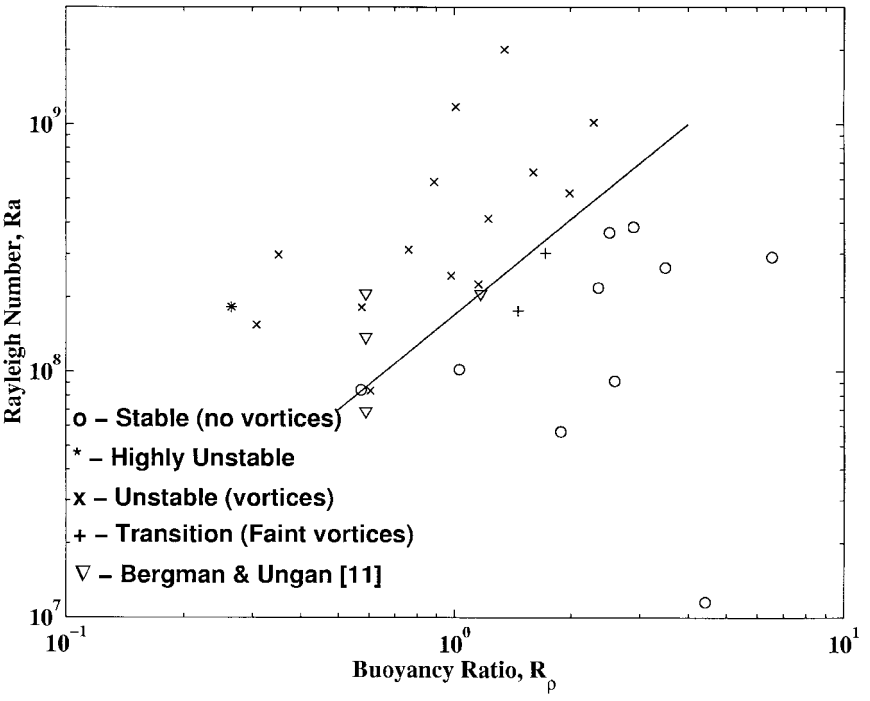

Fig. 9. The lateral Rayleigh number, Ra, as a function of the initial buoyancy ratio, R_ρ. The solid line represents the approximate boundary between stable (below) and unstable (above) experiments.

given Ra, the interfacial vortices disappear as R_ρ is increased. Hence, ΔC has a stabilizing effect on the flow adjacent to the interface.

The present results can be compared with the results of Bergman and Ungan [11] for a box of width $L=10$ cm, and an aspect ratio $A_r=1$ (their experiments D, E, F and M). It should be recalled that our experiments were performed with a slightly different aspect ratio $A_r=0.92$. The results of Bergman and Ungan [11] are represented in Fig. 9 by the triangle symbols (∇). Their data points are located near and above the solid line of Fig. 9, in the regions of transition and unstable experiments. This suggests that the waves that they observed near the interface correspond to the vortices observed in our experiments by the Schlieren technique.

3.5. The mixing time of the two-layer system

An important characteristic of the two-layer system is its lifetime, or, the time until mixing of the two layers is completed. In this work we defined the mixing time as the time elapsed from the start of the lateral heating until the whole fluid was filled with salt fingers (Fig. 3). The mixing time, t_m, was normalized with a characteristic time scale, L^2/D, where D is the coefficient of solute diffusivity and L is the enclosure width. The time scale is chosen with the coefficient of solute diffusivity (and not the heat diffusivity) since mixing of the two layers is associated with the approach of ΔC to zero [11].

The results of the mixing time are presented in Fig. 10, for 25 experiments out of the 27 performed in this work. It is observed in Fig. 10 that the mixing time for the stable (*no vortices*—marked 'o') experiments is, in general, larger than that for the unstable (*vortices*—marked 'x') experiments. This finding can be explained by the enhanced transport of heat and solute across the interface due to the vortices in the unstable experiments. It is in agreement with the result by Bergman and Ungan [11] that for a given R_ρ, the mixing time decreases as Ra is increased.

Straight lines were fitted to the data points in Fig. 10 using the least squares method. The solid line, fitted to the results of the unstable experiments, has a slope of 1.3. The dashed line, fitted to the results of the stable experiments, has a slope of 0.72. Thus, the non-dimensional mixing time, $\tau_m = D \cdot t_m/L^2$ can be expressed as:

$$\tau_m = 0.0025 \times R_\rho^{1.3} \tag{4}$$

for the unstable experiments, and

$$\tau_m = 0.0055 \times R_\rho^{0.72} \tag{5}$$

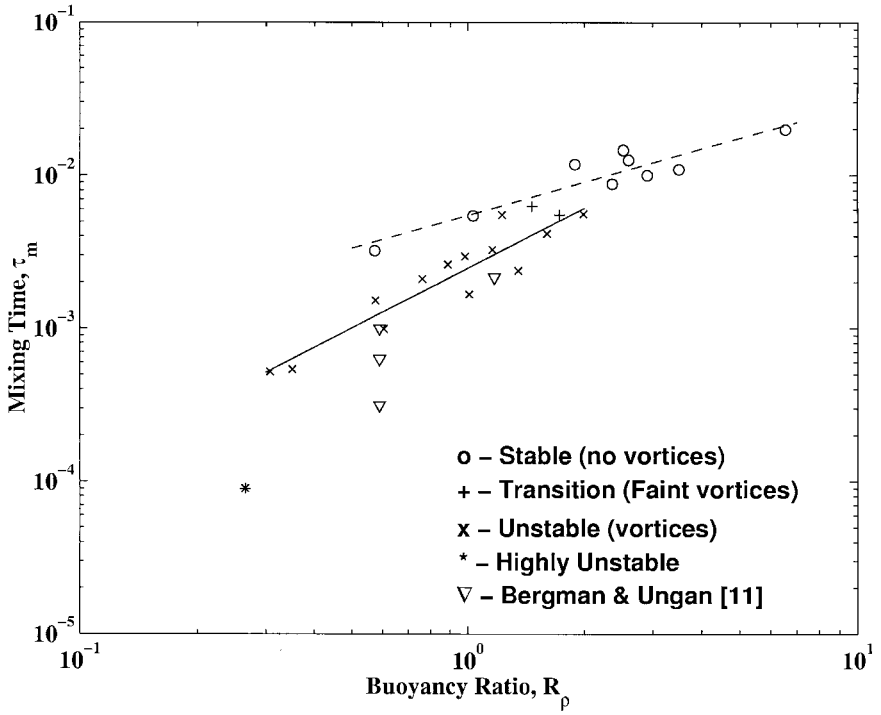

Fig. 10. The non-dimensional mixing time as a function of the initial buoyancy ratio, R_ρ. The dashed line is fitted to the results of the stable experiments while the solid line to the results of the unstable experiments.

for the stable experiments. The accuracy of the mixing time measurement was estimated as ± 2 min. For the unstable experiments this can change the slope of the curve by no more than $\pm 0.8\%$. For the stable experiments, the maximal possible change of the curve slope is $\pm 0.3\%$.

The difference between the slopes of the two curves in Fig. 10 suggests that the transport process across a stable interface is essentially different from the transport process across an unstable interface. In both cases however, the mixing time increases with the buoyancy ratio R_ρ. If ΔC is increased or ΔT is decreased (i.e., R_ρ is increased), the intensity of convection in the system is decreased. Consequently, the rate of salt transport across the interface is reduced and the two-layer system has a longer lifetime.

The mixing time obtained in our experiments can be compared with that measured by Bergman and Ungan [11] (see Section 3.4). Their results are represented on Fig. 10 by the triangle symbols (∇). It is observed that their non-dimensional mixing time is in approximate agreement with the mixing time of the unstable experiments (solid line of Fig. 10) of our study. This supports the observation of Fig. 9, that their experiments were associated with instabilities at the interface region.

4. Concluding remarks

An experimental study was carried out on the mixing of a two-layer stratified system in a laterally heated enclosure. The following conclusions can be drawn from the results of the experiments.

- The appearance of vortices at the interface separating the layers is an instability phenomenon.
- The critical Rayleigh number for the onset of interfacial instabilities increases with the buoyancy ratio of the system.
- For a given R_ρ, the non-dimensional mixing time for *stable* experiments is larger than that for *unstable* experiments.
- For both stable and unstable conditions, the non-dimensional mixing time increases with the buoyancy ratio of the system.

Acknowledgements

The authors thank Mr S. Shargorotski and Mr A. Ashkenazi for their technical assistance with the experimental apparatus. B.Y. is supported by the Israeli Ministry of Absorption. We also thank the executive

of the Center for Technological Education Holon for the financial support in the development of the laboratory.

References

[1] J.S. Turner, Double-diffusive phenomena, Ann. Rev. Fluid Mech. 6 (1974) 37–56.
[2] J.S. Turner, in: Buoyancy effects in fluids, Cambridge University Press, 1979, pp. 251–287.
[3] H.E. Huppert, J.S. Turner, Double-diffusive convection, J. Fluid Mech. 106 (1981) 299–329.
[4] J.S. Turner, Multi-component convection, Ann. Rev. Fluid Mech. 17 (1985) 11–44.
[5] C.F. Chen, D.G. Briggs, R.A. Wirtz, Stability of thermal convection in a salinity gradient due to lateral heating, Int. J. Heat Mass Transfer 14 (1971) 57–65.
[6] R.A. Wirtz, C.S. Reddy, Experiments on convective layer formation and merging in a differentially heated slot, J. Fluid Mech. 91 (3) (1979) 451–464.
[7] J. Tanny, A. Tsinober, The dynamics and structure of double-diffusive layers in side wall-heating experiments, J. Fluid Mech. 196 (1988) 135–156.
[8] J. Tanny, A. Tsinober, On the behavior of a system of double-diffusive layers during its evolution, Phys. Fluids A 1 (3) (1989) 606–609.
[9] S.G. Schladow, E. Thomas, J.R. Koseff, The dynamics of intrusions into a thermohaline stratification, J. Fluid Mech. 236 (1992) 127–165.
[10] E.J. Kranenborg, H.A. Dijkstra, On the evolution of double-diffusive intrusions into a stably stratified liquid: a study of the layer merging process, Int. J. Heat and Mass Transfer 41 (1998) 2743–2756.
[11] T.L. Bergman, A. Ungan, A note on lateral heating in a double-diffusive system, J. Fluid Mech. 194 (1988) 175–186.
[12] M.T. Hyun, T.L. Bergman, Direct simulation of double-diffusive layered convection, ASME J. Heat Trans. 117 (1995) 334–339.
[13] K. Kamakura, H. Ozoe, Double-diffusive natural convection between vertical parallel walls—experimental study of two-layer convection, J. of Chem. Eng. of Japan 24 (5) (1991) 622–627.
[14] K. Kamakura, H. Ozoe, Effect of the temperature dependence of fluid properties on the migration of an interface in double-diffusive natural convection, Int. J. Heat Mass Transfer 38 (18) (1995) 3413–3421.
[15] M.J. Head, The use of miniature four-electrode conductivity probes for high resolution measurements of turbulent density or temperature variations in salt-stratified water flows. PhD thesis, University of California, San Diego 1983.
[16] B.R. Ruddick, T.G.L. Shirtcliffe, Data for double diffusers: physical properties of aqueous salt-sugar solutions, Deep-Sea Res. 26 (A) (1979) 775–787.
[17] R.C. Weast, Handbook of Chemistry and Physics, CRC Press, Cleveland, 1977.
[18] G.K. Batchelor, An Introduction to Fluid Dynamics, Cambridge University Press, 1991.